International Journal of GEOMATE, July 2023, Vol. 25, Issue 107, pp.166-172
ISSN: 2186-2982 (P), 2186-2990 (O), Japan, DOI: https://doi.org/10.21660/2023.107.3851
Geotechnique, Construction Materials and Environment

EFFECTS OF DYNAMIC TRAFFIC LOAD FREQUENCY ON CONSOLIDATION BEHAVIOR OF SOFT CLAY UNDER LOW EMBANKMENT: EXPERIMENTAL AND NUMERICAL INVESTIGATION

*Ngoc Thang Nguyen[1]

[1]Civil and Industrial Construction Division, Faculty of Civil Engineering, Thuyloi University, Vietnam

*Corresponding Author, Received: 03 March 2023, Revised: 26 March 2023, Accepted: 02 April 2023

ABSTRACT: Soft soil is widely distributed over coastal and riverside regions, where the embankment loads are sensitive for differential settlement. In a marine environment, dynamic loading forms a significant proportion of the loading and this decides the safety of many structures founded on the ocean bed. Low embankments may be subjected to dynamic loading in the form of traffic loads, earthquake forces, ocean wave loads, and wind loads. When dynamic cyclic loading is applied, the post-construction settlement of the embankment might increase significantly in comparison with that for static loading, depending upon the magnitude and frequency of the load and the nature of soft soil. This paper used a model of dynamic traffic load to study the effect of cyclic loading frequency on the consolidation behavior of soft clay under low embankments. The experimental results show that the consolidation deformation of the soil samples is independent of the frequency of the dynamic cyclic loading, which was simulated to follow the half-sine wave, and it is consistent with the classic theory of consolidation developed by Terzaghi.

Keywords: Soft soil, Low embankment, Consolidation, Dynamic cyclic loading, Frequency

1. INTRODUCTION

The behavior of soft clay subjected to cyclic loading is important to consider in the design of the low embankment that must resist cyclic loading, because soft clay undergoes greater settlement under cyclic loading than under static loading. Fujiwara and Imran Khan presented laboratory studies on the settlement behavior of soft clay under repetitive loading, which simulated load increment ratio for an oil tank foundation. It was observed that settlement caused by cyclic loading was larger than that caused by static loading and it was larger in the shallow layers than in the deep layers. The difference in compressibility or settlement between these two loading conditions seems to be due to secondary compression and the change in soil particle structures [1, 2]. Favaretti and Yuko presented a simplified consolidation theory under cyclic loading conditions based on Terzaghi's one-dimensional (1-D) consolidation theory. The theory does not only allow estimation of settlement fluctuation with time but also evaluation of the time necessary to reach steady state conditions. The number of load cycles necessary to produce steady-state conditions for low values of T_0, which is duration of a cycle of loading, was much higher in comparison with that for high values of T_0 [3, 4]. Yildirim studied the consolidation settlement of soft clay under cyclic loading for various factors such as the number of cycles and stress level. The consolidation settlement, pore pressure and shear strain were found to decrease after each stage of cyclic loading. The number of cycles is an important parameter that affects the cyclic behavior of soils. The pore pressures and settlement were found to increase with an increasing number of cycles [5]. Jiang investigated the effect of cyclic loading frequency on the dynamic properties of saturated soft marine clay. The research was based on a series of stress-controlled undrained one-way loading cyclic triaxial tests conducted on normally consolidated undisturbed Tianjin soft marine clay. It was found that cumulative axial strain and normalized average pore pressure with a number of cycles are strongly affected by cyclic frequency, but the effect of frequency on normalized average pore pressure with cumulative axial strain is not significant, and the frequency is also a less important factor that affects degradation index with the number of cycles [6].

This study aims at analyzing the impact of dynamic cyclic loading on the degree of consolidation of over-consolidated clay and clarifies the effect of dynamic traffic loading frequency in controlling this settlement increment. The testing procedure is designed to analyze the main factors that affect on the post-construction settlement of embankments, such as the amplitude and frequency of the dynamic cyclic loading.

2. RESEARCH SIGNIFICANCE

The contribution of the study is to demonstrate that the long-term settlement of soft clayey soil the low embankments is independent of the frequency

of dynamic loads, verifying the dynamic cyclic load model theory and providing a basis for evaluating the long-term impact on low embankments subjected to dynamic traffic load.

3. MODEL OF DYNAMIC TRAFFIC LOAD

3.1 Numerical Model of Traffic Load Form

A method for analyzing the behavior of clay under long-term cyclic loading has been proposed by Hyodo and Yasuhara, in which Terzaghi's consolidation equation is proposed for calculating the settlement of low embankment subjected to the traffic load [7, 8]. Hyodo and Yasuhara used a 10-ton truck moving at different speeds of 0km/h, 10km/h, 20km/h, 30km/h, and 35km/h to simulate vehicular load and investigated the vertical stresses acting on top of a subgrade and at different depths of a low embankment. On the subgrade, the vertical stress waveform at some points, shown in Figure 1, can be described as a half-sine curve.

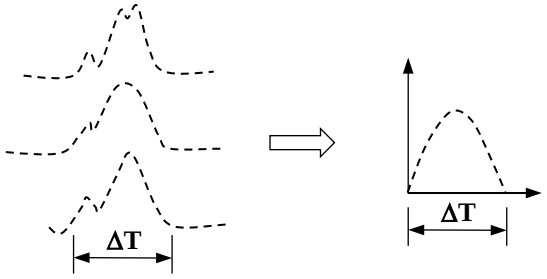

Fig.1 Vertical pressure waveform [7]

Based on the multi-layer elastic theory, Ling and Shoji conducted research on the residual deformation of saturated clay subgrade under vehicular load, analyzing the impact of vehicle speed and loading time without considering the influence of inertia and viscosity on the loading time. Different vehicle speeds of 40km/h, 60km/h, 80km/h, and 100km/h were used to establish an asphalt pavement structure. The experimental results showed that the loading time at any point on top of the subgrade is 0.7205s, 0.4805s, 0.3605s and 0.2885s, respectively. The relationship between vehicle speed and loading time is shown in Figure 2 [9, 10].

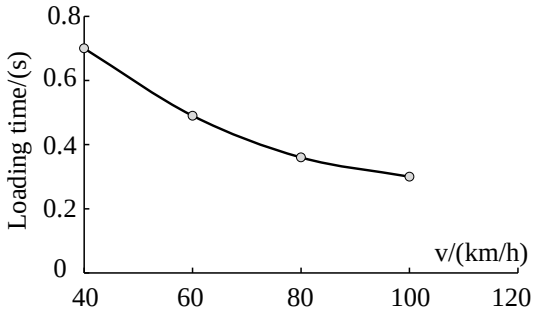

Fig.2 Vehicle speed - Loading time Curve [9, 10].

As shown in Figure 3, the triangular waveform load simulates the vertical stress distribution on top of the subgrade for a typical pavement structure, with a correlation coefficient greater than 0.9. Therefore, the triangular waveform load can be used to simulate the effect of traffic loads on top of the subgrade. In this Figure, the dotted line represents the surface of the subgrade at any point; the solid line is the vertical stress distribution caused by traffic load that affects the surface of the subgrade; the dashed line is the triangular waveform load simulating variation of vertical stresses.

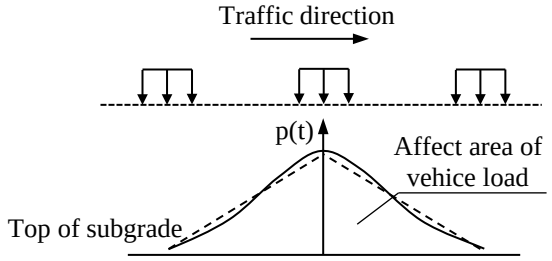

Fig.3 Vertical stress distribution on top of subgrade under vehicular load [9]

Kanghe presented a nonlinear analytical solution for the 1-D consolidation of soft soil under cyclic loading. A soil stratum with thickness H, vertical permeability coefficient k_υ, , volume compressibility coefficient m_υ, and consolidation coefficient C_υ is shown in Fig. 4 [11].

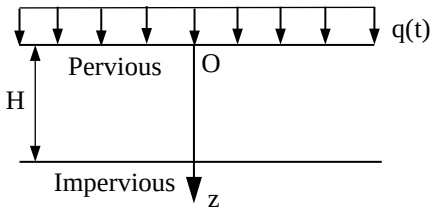

Fig.4 Model of clay layer under cyclic loading [11]

After the elapse of infinite time, the consolidation ratios for loaded periods and unloaded periods at any time, t_1, and depth, z, during loaded periods, T_1, is given by the following equation Eq. (1):

$$U_z = 1 - \frac{4}{\pi}\sum_{m=0}^{\infty}\frac{1}{2m+1}\sin(MZ)\left[\frac{e^{\alpha_m(T_1-t_1)} - e^{\alpha_m(T-t_1)}}{1-e^{\alpha_m T}}\right] \quad (1)$$

Where: T, m is period of time and the number of cycles of cyclic loading respectively; $M=(2m+1)\pi/2$; $Z=z/H$ and $\alpha_m= C_\upsilon(M^2/H^2)$.

From Eq. (1) above, it can be seen that the effect of loading frequency on the degree of consolidation is through the value of T_1 (the loading period) and $(T-T_1)$ (the unloading period). However, after the elapse of infinite time (i.e., $t_1 >> T$), the value of U_z can be obtained as the constant because of:

$$\lim_{t\to\infty}\left[\frac{e^{\alpha_m(T_1-t_1)}-e^{\alpha_m(T-t_1)}}{1-e^{\alpha_m T}}\right]=0 \quad (2)$$

3.2 Cyclic Loading Test Model

Based on the results of previous experimental studies and combining the actual conditions of the vehicular traffic flow and loading characteristics of laboratory equipment, a continuous half-sinusoidal dynamic load waveform is chosen for this study. This takes into consideration a non-continuous load distribution and thus accounts for the distance between vehicles.

The dynamic load waveform is illustrated in Figure 5, where T_1, t_0 are the continuous and interrupted duration of traffic load, respectively. T_1 is the period of time that the dynamic load acted on the soft ground in one cycle. In this model, traffic loads are simulated as a half-sine wave cyclic load. For each test group, the cyclic load frequency, *f*, is constant in order to minimize the differences between the various types of vehicular traffic and their speeds and also to reduce the impact of varying distances between vehicles. P is the sum of vehicle weight and overburden pressure of the embankment; σ_{dmax} is the amplitude of traffic load. The same values of σ_{dmax} are used for a group test, irrespective of the impact of varying sizes of the vehicles.

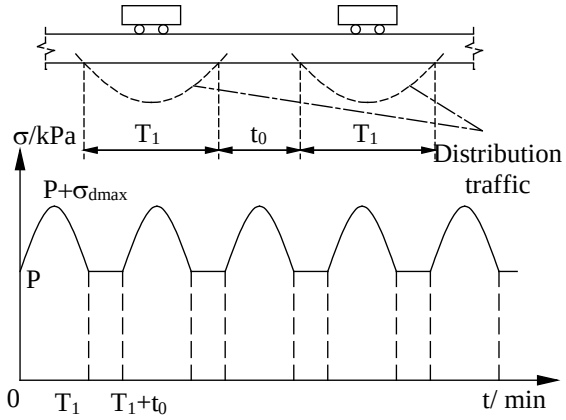

Fig.5 Simulation of the effect of traffic loading

One cycle of loading time includes the acting time of dynamic load T and the interruption time of vehicles t_0, with $t_0>0$. Therefore, as the dynamic load test is simulated to follow the continuous half-sine waveform, load frequency *f* is the inverse of the time period (T) where T reflects the acting time of dynamic traffic load on the subgrade in one cycle. The tests were conducted on 3 sample groups with dynamic cylic load time (T) of 10s, 20s, and 40s corresponding to frequencies of 0.1Hz, 0.05Hz and 0.025Hz, respectively.

3.3. Consolidation Theory Based on the Energy Concept

Guo-Wei Li and Hu studied the effect of dynamic cyclic loading and surcharge preloading method on the settlement of low embankments and showed that the settlement increases with increasing amplitude of cyclic load and the effectiveness of surcharge preloading depends on the difference between the magnitude of surcharge and amplitude of the cyclic load and this is consistent with the energy concept [12- 14].

This study presents selected results of the effects of the frequency on the post-construction settlement of low embankments subjected to cyclic loading. The impact of every load on the soil has been examined as the impact of external energy. Thus the effect of changing frequencies of cyclic loading on the post-construction settlement of embankment on soft ground can be analyzed based on the energy concept. The embankment is assumed to be acted upon by dynamic cyclic loading defined by Eq. (3):

$$\sigma(t)=\sigma_{d\max}\left|\sin\omega t\right| \quad (3)$$

Where σ_{dmax} is the amplitude of load and ω is a parameter of frequency that has a sinusoidal form. From the energy concept, integrating the cyclic loading curve results in the external energy, Eq. (4)

$$Q(t)=\frac{t}{T}\int_0^T\sigma(t)dt \quad (4)$$

Figure 6 shows typical half-sinusoidal curves of cyclic loading with T, the period of one cycle.

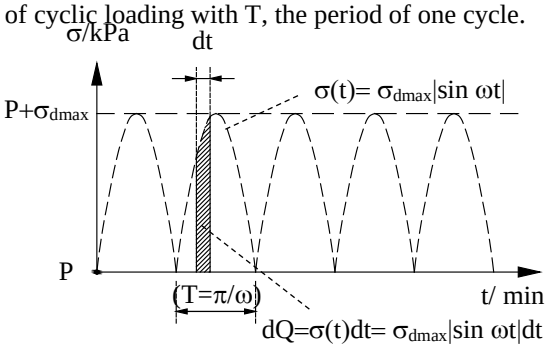

Fig.6 Cyclic loading in typical half-sinusoidal form

Here, the value of T is given by:

$$T=\frac{1}{2}\left(\frac{2\pi}{\varpi}\right)=\frac{\pi}{\varpi} \quad (5)$$

Substituting T from Eq. (5) into the Eq. (3) and combining with Eq. (4), the external energy of cyclic loading is:

$$Q(t)=\frac{1}{(\pi/\varpi)}\int_0^{\pi/\varpi}\sigma_{d\max}\left|\sin\varpi t\right|dt=\frac{2\sigma_{d\max}t}{\pi} \quad (6)$$

From this equation, the external energy imposed on the soil is directly proportional to σ_{dmax} and its acting duration. Also, there is a direct proportionality between stress and strain. Therefore, larger σ_{dmax} and longer acting duration result in higher external energy and, consequently, larger post-construction settlement of the embankment. Further, the external energy equation also shows that the value of Q excludes the variable ω, so the external energy is independent of the frequency of the cyclic loading, and therefore the variation of frequency of the cyclic loading does not affect soil deformation.

4. EXPERIMENTAL STUDIES

4.1 Test Program

4.1.1 Sample and Specimen:

Soil samples were taken from a soft clay deposit located beneath the embankment. The test was conducted on a group of specimens; that had 2 cm and 30 cm^2 height and cross-sectional area, respectively. The main physico-mechanical properties determined from the samples according to standard procedures are shown in Table 1 and the particle size distribution curve for soil samples is shown in Figure 7. All data were determined from tests according to JTG E40-2007 Test Methods of Soils for Highway Engineering.

Table 1 Physico-mechanical properties of soil samples

Physico-mechanical properties		Value
Density ρ (g/cm^3)		1.595
Water Content ω (%)		61.61
Specific Gravity G_s		2.70
Void Ratio e		1.736
Liquid Limit w_l (%)		57
Plastic Limit w_p (%)		32
Plasticity Index I_p		25
Liquidity Index I_L		1.178
Degree of Saturation S_r (%)		98.9
Compression Factor $\alpha_{0.1\text{-}0.2}$ (MPa^{-1})		1.372
Compression Modulus E_s (MPa)		1.356
Coefficient of consolidation	C_{v100}	0.391
	C_{v200}	0.487

In here: C_{v100} ($10^{-3}cm^2/s$) and C_{v200} $10^{-3}cm^2/s$: correspond with the pre-consolidation stresses of 100kPa and 200kPa, respectively.

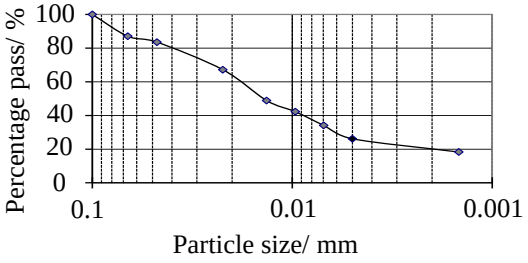

Fig.7 The particle size distribution

4.1.2 Test Procedure:

The samples were subjected to one dimension consolidation test in which static loads, P or dynamic cyclic loads of amplitude, $\sigma_{d\max}$ were applied. The loading procedure for cyclic load tests is as follows. In the first loading step, the specimens were consolidated under a sustained load of 25 kPa for 2 hours; in the second loading step, the specimens were consolidated under sustained loads of 200 kPa for 24 hours; in the third loading step, the consolidation pressure was reduced to 180 kPa, and then was kept under that load for 24 hours; in the final loading step, the specimens were consolidated under the additional cyclic loads of 7, 13 and 20 kPa for a week. In the cyclic consolidation tests, the loading, which varied with different frequencies, was simulated to follow the half-sine wave. The loading scheme of group specimens is summarized in Table 2.

Table 2 Summary of test scheme

Test type	P (kPa)	ΔP (kPa)	σ_{dmax} (kPa)	f (Hz)
Static	200	20	0	0
	180	20	0	0
Dynamic	180	20	7	0.1
	180	20	7	0.05
	180	20	7	0.025
	180	20	13	0.1
	180	20	13	0.05
	180	20	13	0.025
	180	20	20	0.1
	180	20	20	0.05
	180	20	20	0.025

The loading apparatus consists of three main components: the stress sensors, controller and loading device; the schematic and picture of the apparatus in the test are shown in Figure 8 (a-c) below.

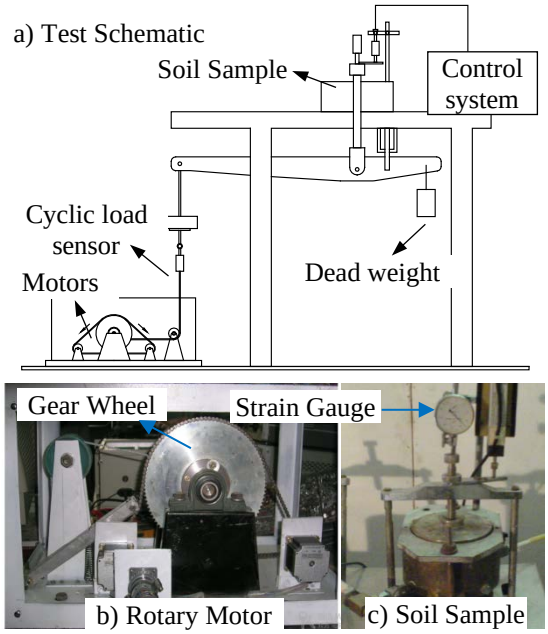

Fig.8 Pictures of Apparatus Used in the Test

5. RESULTS AND ANALYSIS

5.1 Vertical Strain-Time Curves

Figure 9(a-b) shows the variability of vertical strain with time for both the cyclic tests with the frequency of 0.05Hz, and the static tests. In Figure 9a, the relationship between strain and normal time would not be linear when the curves are plotted for all the points. But in Figure 9b there is an approximately linear relationship between the strain and the logarithm of elapsed time.

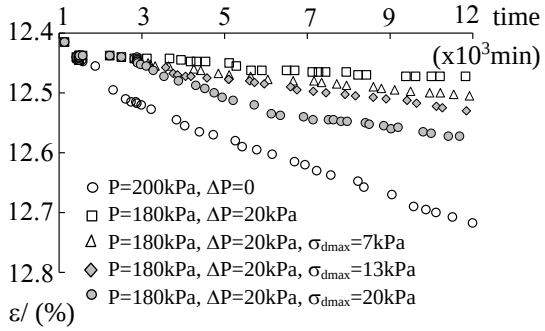

Fig.9a Strain- time curves

The vertical strain increased with increasing σ_{dmax}, and elapsed time (t). $\Delta\varepsilon$ values of 0.09%, 0.15% and 0.25% were obtained for σ_{dmax} values of 7, 13 and 20 kPa, respectively, at the end of the loading period. Similar results were obtained for frequencies of 0.025 and 0.10Hz. Thus, the post-construction settlement of the embankment is larger under the effect of cyclic loading than under static loading, and the higher amplitude corresponds with the higher settlement.

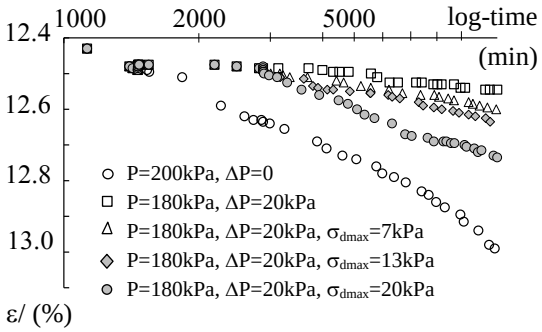

Fig.9b Strain-log(time) curves

5.2 Effect of the Cyclic Loading Frequency on Strain History

Figure 10 illustrates the relationship between the difference in strain (i.e., difference between strains caused by P+σ_d and P) and cyclic loading with different σ_d and frequencies, *f*, for test samples, in which the frequency of cyclic loading varies continuously according to sinusoidal form.

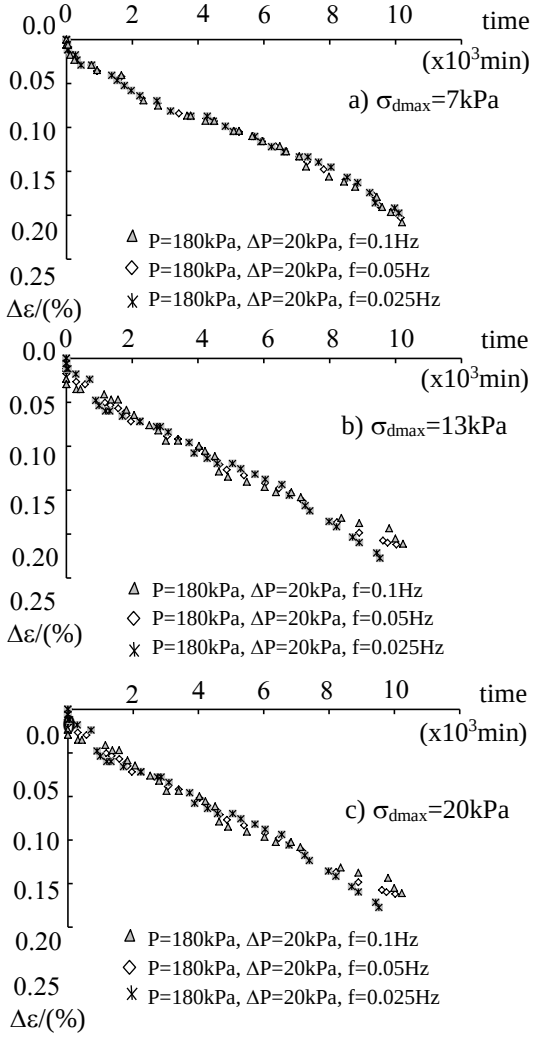

Fig.10 Strain histories for the test scheme

In the figures, the application of the cyclic loading on the samples starts from the origin, and the strain increases linearly with time. Figure 10 also shows that although the frequencies of cyclic loading are different, the strain curves are quite similar; the difference is insignificant. Thus the change in of strain of test samples is independent of the frequency of the cyclic loading. This phenomenon is consistent with the external energy in Eq (6).

5.3 Degree of Consolidation

Figure 11 illustrates the comparison of the degree of consolidation histories for the test scheme. This Figure shows that although the frequencies of cyclic loading are different, the curves are quite similar, and the difference is insignificant. Thus the change in the degree of consolidation of test samples is independent of the frequency of the cyclic loading.

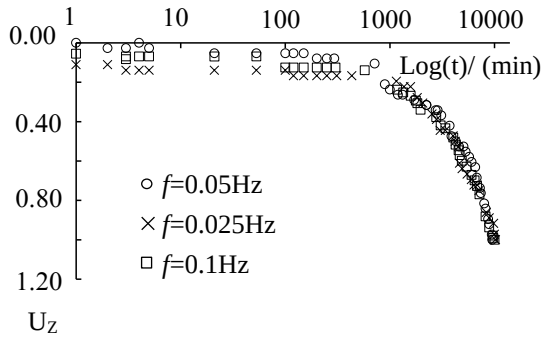

Fig.11 Degree of consolidation, U_z

Figure 12 (a-c) display the degree of consolidation, U_z, versus time results for the cyclic loading tests with the different value of frequency f of 0.025Hz, 0.05Hz and 0.1Hz.

These theoretical formula curves have been plotted based on Terzaghi's theory's equations for a uniform square wave of cyclic loading. Here, the equations are applied for theoretical analysis by Eq. (1) and Eq. (2), in which the value of T and t_1 were calculated based on the energy principle of equivalence with the oedometer creep test. The test was conducted on 3 sample groups corresponding to time (T) of 10s, 20s, and 40s, corresponding to cyclic load frequencies, f, (i.e., the inverse of T) of 0.1Hz, 0.05Hz and 0.025Hz, respectively.

6. CONCLUSIONS

One dimension (1-D) consolidation of a saturated soil subjected to cyclic loading have great signification in estimating the total post-construction settlement of low embankment. The consolidation settlement of the soil is independent of the frequency of the dynamic cyclic loading, which was simulated to follow the half-sinusoidal form, and it is consistent with the energy concept. The distribution of the theoretical consolidation curves for dynamic loading is fairly consistent with the cyclic loading test results.

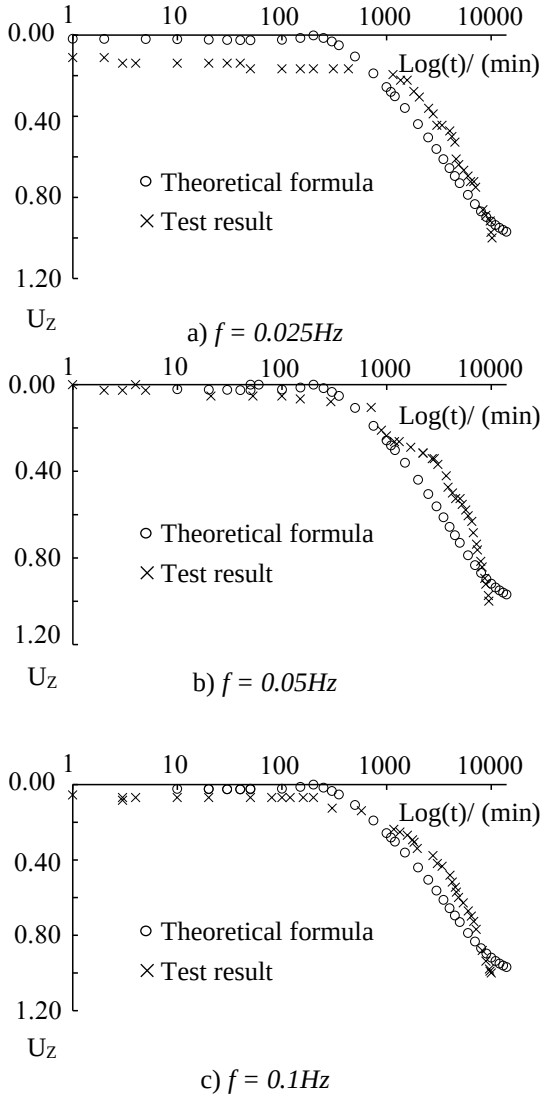

Fig.12 Degree of consolidation, U_z, for test scheme with the frequency of 0.025Hz, 0.05Hz and 0.1Hz

7. REFERENCES

[1] Fujiwara H., and Ue S., Effect of preloading on post-construction consolidation settlement of soft clay subjected to repeated loading. Soils and Foundations, Vol. 30, Issue.1, 1990, pp. 76-86.

[2] Imran K., Kentaro N., and Toshihiro N., Undrained cyclic shear behavior of clay under drastically changed loading rate. International Journal of GEOMATE, Vol.18, Issue 66, 2020, pp. 16-23.

[3] Favaretti M., and Soranzo M., A simplified consolidation theory in cyclic loading conditions. Proc. of Int. Symposium on Compression and Consolidation of Clayey Soils, Japan, Vol. 3, 1995, pp. 405-409.

[4] Yuko I., Ayaka O., Weerakaset S., Chalemnchai T., Chaweewan D., Masamitsu F., and Ryoichi F., Estimation of initial void ratio of consolidated clay based on one-dimensional consolidation theory. Journal of GEOMATE, Vol.14, Issue 46, 2018, pp. 51-56.

[5] Yildirim H., and Er-San H., Settlements under consecutive series of cyclic loading. Soil Dynamics and Earthquake Engineering, Vol. 27, Issue.6, 2007, pp. 577-585.

[6] Jiang M., Cai Z., Cao P., and Liu D., Effect of Cyclic Loading Frequency on Dynamic Properties of Marine Clay. Soil Dynamics and Earthquake Engineering, GeoShanghai International Conference, 2010, pp. 240-245.

[7] Hyodo M., and Yasuhara K., Analytical procedure for evaluating pore-water pressure and deformation of saturated clay ground subjected to traffic loads. Proceedings of the sixth international conference on numerical methods in geomechanics, Innsbruck, Austria, Vol. 1, Issue 3, 1988, pp. 653-658.

[8] Yasuhara K., Hirao K. and Kato S., Cyclic induced settlement in soft clay. 8th European Conf, SMFE, Vol. 1, 1991, pp. 887- 890.

[9] Ling J. M., Wang W., and Wu H. B., On Residual Deformation of Saturated Clay Subgrade under Vehicle Load. Journal of TongJi University, Vol. 3, Issue 11, 2002, pp. 1315- 1320.

[10] Shoji K., A prediction method for long-term settlement of higly organic soft soil. International Journal of GEOMATE, Vol.17, Issue 60, 2019, pp.162-169.

[11] Kanghe X., Kun W., Guohong C., and Anfeng H., One-dimensional consolidation of over consolidated soil under time-dependent loading. Frontiers of Architecture and Civil Engineering in China, Vol. 2, Issue 1, 2008, pp. 67-72.

[12] Guo-Wei L., Thang N. N., and Andrew C. A., Settlement Prediction of Surcharge Preloaded Low Embankment on Soft Ground Subjected to Cyclic Loading. Marine Georesources & Geotechnology, Vol. 34, Issue 6, 2016, pp.154-161.

[13] Li G. W., Li X., Ruan Y. S., Hou Y. Z., and Yin J. H., Creep model of over-consolidated soft clay under plane strain. Chinese Journal of Rock Mechanics and Engineering, Vol. 35, Issue 11, 2016, pp.2307–2315.

[14] Hu Y. Y., Yang P., and Yu Q. Z., Time effect of secondary consolidation coefficient of over-consolidated soil. China Journal of Highway and Transport, Vol. 29, Issue 9, 2016, pp. 29–37.